HELICOPTER ROTOR AEROELASTIC STABILITY EVALUATION USING LYAPUNOV EXPONENTS

Aykut Tamer, Pierangelo Masarati

Department of Aerospace Science and Technology, Politecnico di Milano
via La Masa 34, 20156 - Milano, ITALY
{aykut.tamer,pierangelo.masarati}@polimi.it

Abstract

This work presents the application of Lyapunov Characteristic Exponents (LCEs), or in short Lyapunov Exponents, to the evaluation of rotorcraft aeroelastic stability. Current state of art literature on rotorcraft aeroelastic stability analysis approaches the problem by either using a constant coefficient approximation or by computing the eigenvalues of the monodromy matrix according to Floquet Theory. The former neglects periodicity and the latter is only applicable to the perturbation of the problem about a periodic orbit. Often such approximations are acceptable; however, LCEs can be applied to generic trajectories of non-linear systems to produce an estimate of the stability properties without the need to reach a steady orbit or determine the period of the system. Being more general, LCEs can provide a common environment in rotorcraft aeroelastic stability among both linear and non-linear systems, and be applicable to all problems that can be proficiently analyzed by time marching analysis, including experimental data. This work presents the evaluation of the stability of an isolated rotor formulated as a linear time-periodic system by computing the LCEs from arbitrary fiducial trajectories. The method is illustrated in relation with the problem of rigid helicopter blade flapping, and ground resonance with one damper inoperative and with non-linear dampers.

1. INTRODUCTION

The stability of a dynamical system is related to the evolution of a solution after perturbation. The practical, quantitative way of measuring stability depends on whether a system is autonomous (i.e. not explicitly dependent on time) and linear. Stability of linear, time invariant (LTI) systems can simply be inferred by computing the eigenvalues of the state space matrix, namely its spectrum. The problem is more complex when the system is linear non-autonomous, but time periodic (LTP), i.e. the state space matrix has periodic coefficients. The stability of LTP systems is evaluated by computing the eigenvalues of the monodromy matrix, namely the state transition matrix over one period. For non-linear, autonomous problems, the eigenvalues and eigenvectors of the linearized system computed at the coordinates of the phase plane corresponding to a steady solution provides the local information about the behavior of the system in the neighborhood of that solution. Once these points are evaluated and connected for the whole phase plane, geometric understanding of the system is possible. However, for problems having higher dimensions geometric understanding is not so easy and quantitative way of measuring is necessary.

LTI and LTP problems typically result from linearization of non-linear, non-autonomous problems about a steady (both LTI and LTP) or a periodic (LTP only) reference solution. They require the existence of such solution, and the capability to define and compute it. Obtaining a steady or periodic solution by numerical integration in time requires that solution to be stable, so the study of the stability of the solution is actually the study of *how much stable it is*, i.e. of its stability margin.

A method that does not require a special reference solution (i.e. a stable point or a stable orbit) but, on the contrary, provides indications about the existence of an *attractor*, being it a point, a periodic orbit or a higher-order solution (e.g. a multidimensional torus), while computing the evolution of the system towards it, would give valuable insight into the system properties and, at the same time, provide a viable and practical means for its analysis.

Lyapunov Characteristic Exponents (LCE) or in short Lyapunov Exponents are indicators of the nature and of the stability properties of solutions of differential equations (see for example Refs.[1, 2] and references therein). They define the spectrum of the related Cauchy (initial value) problem. Lyapunov theory can be applied to non-linear non-autonomous systems. The

stability of trajectories in state space can be estimated while computing their evolution.

Both LTI and LTP find several applications in the analysis of problems related to rotary-wing aircraft as a consequence of the intrinsic periodicity of rotor motion[1]. Moreover, non-linearity always present in any dynamical system including rotorcraft, and should be checked for stability. This work presents the use of LCEs in analyzing rotorcraft stability that is believed to provide a common stability analysis platform for dynamical rotorcraft systems having different levels of complexity. The method is demonstrated on well-known rotorcraft problems. Rigid helicopter blade flapping and helicopter ground resonance problems are chosen as LTP cases and LCEs are compared with the results obtained using Floquet Theory. Moreover LCEs of a non-linear problem is estimated by introducing non-linear dampers to helicopter ground resonance problem.

2. Lyapunov Characteristic Exponents

This section recalls the definition of non-autonomous problems and of the so-called Lyapunov Characteristic Exponents as a measure of its spectrum and the numerical procedure used in this study for their estimation.

2.1 Non-Autonomous Problems

In engineering practice, differential problems of the form

$$\dot{\mathbf{x}} = \mathbf{f}(\mathbf{x}, t), \qquad \mathbf{x}(t_0) = \mathbf{x}_0 \tag{1}$$

arise often. Special cases occur when the problem is linear, i.e. $\mathbf{f}(\mathbf{x}, t) = \mathbf{A}(t)\mathbf{x}(t)$, or even periodic, i.e. linear with $\mathbf{A}(t + T) = \mathbf{A}(t)$ for a given constant T, $\forall t$. Autonomous problems arise when $\mathbf{f}(\mathbf{x})$ does not explicitly depend on time t; a special case occurs when the problem is linear, i.e. $\mathbf{f}(\mathbf{x}) = \mathbf{A}\mathbf{x}$. In the latter case, the spectrum of the problem is clearly represented by the eigenvalues of matrix $\mathbf{A}$. In the other cases, its definition is less intuitive. Yet, the rate of decay of the amplitude of the trajectory with respect to initial perturbations, i.e. *stability* , have the same interpretation and they are quantitatively comparable. This corresponds to the real part of eigenvalues of matrix $\mathbf{A}$ for a LTI system, logarithm of the real part of eigenvalues of matrix monodromy matrix for an LTP problem and as it is shown here LCEs for any problem including non-linear and non-autonomous problems.

[1]Strictly speaking, periodic problems only occur under strict assumptions; for example, the motion of a helicopter is periodic only during idealized steady, coordinated maneuvers.

2.2 Lyapunov Exponents

Given the problem $\dot{\mathbf{x}} = \mathbf{f}(\mathbf{x}, t)$, with the state $\mathbf{x} \in \mathbb{R}^n$, the time $t \in \mathbb{R}$, and the nonlinear function $\mathbf{f} \in \mathbb{R}^{n+1} \to \mathbb{R}^n$, and a solution $\mathbf{x}(t)$ for given initial conditions $\mathbf{x}(0) = \mathbf{x}_0$, the Lyapunov Characteristic Exponents λ_i are defined as[2]

$$\lambda_i = \lim_{t\to\infty} \frac{1}{t} \log \|{}_i\mathbf{x}(t)\|, \tag{2}$$

where ${}_i\mathbf{x}(t)$ is the solution that describes the exponential evolution of the i-th axis of the ellipsoid that grows from an initially infinitesimal n-sphere according to the map $\mathbf{f}_{/\mathbf{x}}$ tangent to $\mathbf{f}$ along the fiducial trajectory $\mathbf{x}(t)$, i.e. the solution of the linear, non-autonomous problem ${}_i\dot{\mathbf{x}}(t) = \mathbf{f}_{/\mathbf{x}}(\mathbf{x}(t), t)\, {}_i\mathbf{x}(t)$, with ${}_i\mathbf{x}(t_0) = {}_i\mathbf{x}_0$. The definition involves the limit for $t \to \infty$; hence, in practice LCEs can only be numerically estimated for a sufficiently large value of t. In this study, unless explicitly stated, with the term "LCEs" we refer to their estimation using a large enough value of t.

LCEs represent a measure of the rate of growth of perturbed solutions. Consider infinitesimal, independent perturbations of the states with respect to a solution $\mathbf{x}(t)$ of Eq. (2) (the fiducial trajectory). The perturbed solution can be computed in terms of the state transition matrix $\mathbf{\Phi}(t, t_0)$, considering $\mathbf{A}(\mathbf{x}, t) = \mathbf{f}_{/\mathbf{x}}$, as the solution of the problem

$$\dot{\mathbf{\Phi}}(t, t_0) = \mathbf{A}(\mathbf{x}, t)\mathbf{\Phi}(t, t_0), \qquad \mathbf{\Phi}(t_0, t_0) = \mathbf{I}. \tag{3}$$

According to the Ostrogradskiĭ-Jacobi-Liouville formula,[1] the determinant of $\mathbf{\Phi}(t, t_0)$ (the *Wronskian determinant* of the independent solutions that constitute $\mathbf{\Phi}(t, t_0)$) is

$$\det(\mathbf{\Phi}(t, t_0)) = \det(\mathbf{\Phi}(t_0, t_0))\, \mathrm{e}^{\int_{t_0}^{t} \mathrm{tr}(\mathbf{A}(\tau))\ \mathrm{d}\tau}, \tag{4}$$

where $\mathrm{tr}(\cdot)$ is the trace operator. Thus, the Wronskian never vanishes when $\mathbf{A}(t)$ is regular in $[t_0, t]$, since $\mathbf{\Phi}(t_0, t_0) \equiv \mathbf{I}$. The Wronskian geometrically represents the evolution in time of the volume of an infinitesimal portion of the state space.

The evolution of an arbitrary perturbation ${}_i\mathbf{x}(t_0) = {}_i\mathbf{x}_0$ is ${}_i\mathbf{x}(t) = \mathbf{\Phi}(t, t_0)\, {}_i\mathbf{x}_0$. As such, the contraction or expansion rate along the direction of ${}_i\mathbf{x}$ is estimated by considering

$$\left(\mathrm{e}^{\chi_i t}\right)^2 = \lim_{t\to\infty} \frac{{}_i\mathbf{x}^T\, {}_i\mathbf{x}}{{}_i\mathbf{x}_0{}^T\, {}_i\mathbf{x}_0}. \tag{5}$$

Consider now the singular value decomposition (SVD) of $\mathbf{\Phi}(t, t_0)$,

$$\mathbf{U}\mathbf{\Sigma}\mathbf{V}^T = \mathbf{\Phi}(t, t_0), \tag{6}$$

[2]Actually, Eq. (2) should be

$$\lambda_i = \lim_{t\to\infty} \frac{1}{t} \log \frac{\|{}_i\mathbf{x}(t)\|}{\|{}_i\mathbf{x}(t_0)\|};$$

however, one can easily prove that for any non-zero constant c the LCE of $cf(x, t)$ is equal to the LCE of $f(x, t)$.

where $\mathbf{U} = \mathbf{U}(t)$ and $\mathbf{V} = \mathbf{V}(t)$ are orthogonal matrices. The singular values σ_i, namely the diagonal elements of $\mathbf{\Sigma} = \mathbf{\Sigma}(t)$, which are strictly greater than zero as a consequence of the above mentioned Ostrogradskiĭ-Jacobi-Liouville formula[3], Eq. (4), express the growth of the perturbed solution along orthogonal directions in the state space.

The LCEs can also be interpreted as the limit for $t \to \infty$ of the logarithm of the singular values, σ_i, divided by the time itself[2][4]. In fact, using the SVD to express the state transition matrix, Eq. (5) becomes

$$\left(\mathrm{e}^{\chi_i t}\right)^2 = \lim_{t\to\infty} \frac{{}_i\mathbf{x}_0{}^T \mathbf{V}\mathbf{\Sigma}^2\mathbf{V}^T {}_i\mathbf{x}_0}{{}_i\mathbf{x}_0{}^T {}_i\mathbf{x}_0} \tag{7}$$

and independently considering perturbations ${}_i\mathbf{x}_0$ along the directions represented by the columns of $\mathbf{V}$, ${}_i\mathbf{x}_0 = \mathbf{V}_i$, one obtains

$$\chi_i = \lim_{t\to\infty} \frac{\log(\sigma_i)}{t} = \lambda_i. \tag{8}$$

So-called continuous formulas for the estimation of the LCEs can be derived from the definition based on the SVD, as well as on the QR decomposition (see for example[3]). Such formulas suffer from the numerical difficulty of dealing with matrices whose coefficients either rapidly converge to zero (exponential stability) or diverge (instability). For this reason, different approaches have been formulated; the so-called discrete QR method, based on the incremental use of the QR decomposition of the state transition matrix for each time step, is discussed in the next section.

2.3 The Discrete QR Method

The definitions of Eqs. (2) and (8) can hardly be applied to the practical estimation of LCEs, because some sort of orthogonalization is needed to prevent the solution for each axis of the ellipsoid from interfering with the others. Numerical methods have been devised for this purpose. One of the most popular is the so-called Discrete QR method, which is based on incrementally updating the LCEs estimates with the diagonal elements of matrix $\mathbf{R}$ obtained from the QR decomposition of the state transition matrix between two consecutive time steps.

Given the state transition matrix $\mathbf{Y}(t, t_{j-1})$ from time t_{j-1} to an arbitrary time t as the solution of the problem $\dot{\mathbf{Y}} = \mathbf{f}_{/\mathbf{x}}(\mathbf{x}(t), t)\mathbf{Y}$ with $\mathbf{Y}(t_{j-1}, t_{j-1}) = \mathbf{I}$, set $\mathbf{Y}_j = \mathbf{Y}(t_j, t_{j-1})$. Consider then the QR decomposition of $\mathbf{Y}_j\mathbf{Q}_{j-1}$, which implies $\mathbf{Q}_j\mathbf{R}_j = \mathbf{Y}_j\mathbf{Q}_{j-1}$. Now, after defining $\mathbf{R}_{\Pi_j} = \Pi_{k=0}^{j}\mathbf{R}_{j-k}$, one can show that

$$\mathbf{Y}_j\mathbf{Q}_{j-1}\mathbf{R}_{\Pi_{j-1}} = \mathbf{Q}_j\mathbf{R}_j\mathbf{R}_{\Pi_{j-1}} = \mathbf{Q}_j\mathbf{R}_{\Pi_j} \tag{9}$$

This way, $\mathbf{Y}_j\mathbf{Q}_{j-1}\mathbf{R}_{\Pi_{j-1}}$ can be used to construct $\mathbf{R}_{\Pi_j}$ by only considering incremental QR decompositions over $\mathbf{Y}_j\mathbf{Q}_{j-1}$, i.e. with limited contraction/expansion. The LCEs are then estimated from $\mathbf{R}_{\Pi_j}$ as

$$\lambda_i = \lim_{j\to\infty} \frac{1}{t_j} \log r_{ii}(t_j), \tag{10}$$

where $j \in \mathbb{N}$ and $r_{ii}(t_j)$ are the diagonal elements of matrix $\mathbf{R}(t_j) = \mathbf{R}_{\Pi_j}$. Since the product of two upper triangular matrices $\mathbf{C} = \mathbf{AB}$ is also an upper triangular matrix, whose diagonal elements are $c_{ii} = a_{ii}b_{ii}$. Thus the logarithm of c_{ii} can be incrementally computed as $\log(a_{ii}b_{ii}) = \log(a_{ii}) + \log(b_{ii})$. This helps preventing overflow/underflow in numerical computations. Furthermore,

$$r_{ii}(t_j) = \Pi_{k=0}^{j} r_{(j-k)_{ii}}, \tag{11}$$

thus

$$\log\left(r_{ii}(t_j)\right) = \sum_{k=0}^{j} \log(r_{k_{ii}}), \tag{12}$$

which leads to

$$\lambda_i = \lim_{j\to\infty} \frac{1}{t_j} \sum_{k=0}^{j} \log(r_{k_{ii}}). \tag{13}$$

2.4 Computation of State Transition Matrix

The state transition matrix is required in discrete QR decomposition method; hence, numerical integration is necessary to obtain it. For a small enough time step, Eq. (1) is linearized,

$$\boldsymbol{\delta}\dot{\mathbf{x}} = \mathbf{A}(\mathbf{x}(t), t)\boldsymbol{\delta}\mathbf{x} \tag{14}$$

where $\mathbf{A} = \mathbf{f}_{/\mathbf{x}}$, partial derivative of non-linear function $\mathbf{f}$ with respect to state space variables $\mathbf{x}$. Generally, since $\mathbf{f}$ can be any non-linear function of the trajectory $\mathbf{x}_j$ and time t, the integration of the state transition matrix requires the knowledge of the trajectory. Computing the fiducial trajectory is not specifically addressed in this context; the computation of the state transition matrix is discussed for clarity. In this study, two methods are considered for the practical computation of the state transition matrix. The *One-leg trapezoid rule* is used to compute the state transition matrix for all types of problems from linear to non-linear time variant. *Hsu's Method* is also used for linear problems.

[3] When $\mathbf{\Phi}(t_0, t_0) = \mathbf{I}$ is chosen, its determinant is 1; the integral of matrix $\mathbf{A}(t)$ is finite, and thus its exponential is a strictly positive number.

[4] In,[2] the actual definition is

$$\lambda_i = \lim_{t\to\infty} \frac{\log(\sigma_i^2)}{2t},$$

where σ_i^2 are the eigenvalues of $\mathbf{\Phi}^T(t, t_0)\mathbf{\Phi}(t, t_0) = \mathbf{V}\mathbf{\Sigma}^2\mathbf{V}^T$.

One-Leg Trapezoid Rule Integration: As explained in,[4] under the assumption that a constant integration time step h is used, state $\mathbf{x}$ and its derivative $\dot{\mathbf{x}}$ at time t_j can be defined respectively as the average of and the difference between the values of the state $\pm$ half of the time step forward and backward

$$\mathbf{x}_j = \frac{\mathbf{x}_{j+1/2} + \mathbf{x}_{j-1/2}}{2}, \tag{15a}$$

$$\dot{\mathbf{x}}_j = \frac{\mathbf{x}_{j+1/2} - \mathbf{x}_{j-1/2}}{h} \tag{15b}$$

This corresponds to using a one-leg trapezoid rule-like approximation of the state and its derivative. Eq. (15) at time t_j, using the expressions of $\mathbf{x}_j$ and $\dot{\mathbf{x}}$ from Eq. (14), and solved for $\mathbf{x}_{j+1/2}$, yields

$$\mathbf{x}_{j+1/2} = \left(\mathbf{I} + \frac{h}{2}\mathbf{A}_j\right)^{-1} \left(\mathbf{I} - \frac{h}{2}\mathbf{A}_j\right) \mathbf{x}_{j-1/2} \tag{16}$$

implies

$$\mathbf{Y}_j = \left(\mathbf{I} + \frac{h}{2}\mathbf{A}_j\right)^{-1} \left(\mathbf{I} - \frac{h}{2}\mathbf{A}_j\right) \tag{17}$$

This equation is required to be integrated together with Eq. (1) if $\mathbf{f}$ is nonlinear. For LTI systems, the state transition matrix is independent of the trajectory $\mathbf{x}(t)$, hence there is no need to integrate Eq. (1).

Integration Using Hsu's Method: When Hsu's method[5] is used to compute the state transition matrix of Linear Time Variant (LTV) (and the special case of Linear Time Periodic, LTP) problems, the formulation can be written in a more compact form.

The method applies to LTV problems of the form $\dot{\mathbf{x}} = \mathbf{A}(t)\mathbf{x}$ by considering a piecewise constant approximation of matrix $\mathbf{A}(t)$, namely $\mathbf{A}(t) \approx \mathbf{A}(\hat{t}) = \hat{\mathbf{A}}$ with $\hat{t} \in [t_j, t_{j+1}]$, where $t_j \leq t \leq t_{j+1}$. The choice of $\hat{t}$ may influence the results. Then, the state transition matrix is readily obtained as

$$\mathbf{Y}(t, t_j) \approx \mathrm{e}^{\hat{\mathbf{A}}(t-t_j)}, \tag{18}$$

where the matrix exponential may be approximated (e.g. truncated when computed as a matrix power series) to improve the computational efficiency of the method.

3. Numerical Examples

This section presents numerical applications of the proposed procedure. Most of them are related to Linear Time Periodic (LTP) problems because such problems, although linear, require special methods for stability evaluation (i.e. Floquet theory) and, as such, provide the opportunity to compare results. Specifically, the stability of solutions of a LTP problem can be evaluated using Floquet's theory, by checking the eigenvalues of the monodromy matrix. The applications are related to helicopters, and present a clear source of periodicity, non-linearity, and a variety of stability issues.

3.1 Helicopter Blade Flapping

Rigid blade flapping can be considered as a second order single degree of freedom Linear Time Periodic problem (from Ref.[6]) under simplifying assumptions. Since the purpose of this example is to address LTP systems, rather than using a more realistic but complex helicopter blade dynamics model only periodicity is retained, and the model is oversimplified by linearizing the dynamics, using quasi-static aerodynamics and neglecting reverse flow conditions. Considering the dots represent differentiation with respect to t, where t is the azimuth angle (in this context it represents non-dimensional time), the equation of motion can be written as,

$$\ddot{\beta} + \frac{\gamma}{8}\left(1 + \frac{4}{3}\mu\sin(t)\right)\dot{\beta} + \left(\nu_\beta^2 + \frac{\gamma}{8}\left(\frac{4}{3}\mu\cos(t) + \mu^2\sin(2t)\right)\right)\beta = 0 \tag{19}$$

that represents the flapping of a rigid helicopter blade, where β is the blade flap angle, γ is the Lock number (the non-dimensional ratio between aerodynamic and inertial flapping loads, which in the present context loosely represents the damping factor), μ is the advance ratio (the ratio between the helicopter forward velocity and the blade tip velocity in hover, which weighs the periodic part of the coefficients) and ν_β is the non-dimensional flapping frequency. In order to demonstrate the trend of LCE estimates for a range of parameter, the advance ratio μ is chosen as the parameter.

Clearly, a trivial fiducial trajectory is $\beta(t) = 0$, which is obtained for $\beta(0) = 0$ and $\dot{\beta}(0) = 0$. Other non-trivial trajectories can be obtained starting from arbitrary initial conditions; were $\beta(t) = 0$ asymptotically stable, the solution converges on it. Since this problem is linear and homogeneous, $\beta(t) = 0$ is the unique equilibrium point and stability does not depend on the initial conditions.

The problem is rewritten in first order form,

$$\left\{ \begin{array}{c} \dot{\beta} \\ \ddot{\beta} \end{array} \right\} = \left[\begin{array}{cc} 0 & 1 \\ K_\beta & C_\beta \end{array} \right] \left\{ \begin{array}{c} \beta \\ \dot{\beta} \end{array} \right\}, \tag{20}$$

and integrated to compute the state transition matrix at each time step. LCEs are estimated according to the proposed approach. The evolution of LCE estimates in non-dimensional time, associated with complex conjugate eigenvalues is shown in Fig. 1: at the top starting from the time when the system is initially perturbed and at the bottom the behavior is zoomed for large enough value of t.

Owing to periodicity, the mean value of the two LCE estimates when Floquet characteristic values are complex conjugate shows a decaying oscillatory behavior with the period of the system, $T = 2\pi$. The decay is

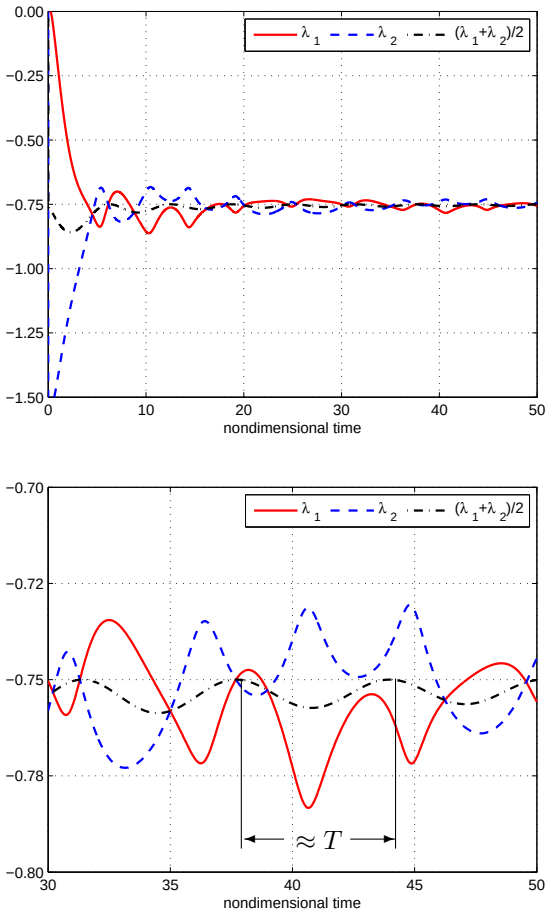

Figure 1: Blade flapping: nondimensional time evolution of LCE estimates associated with complex conjugate eigenvalues; time history (top) and zoom after convergence (bottom).

caused by the division by t in accordance with Eq. (2). In order to have an accurate estimate of the LCEs, integration needs to be performed for a large enough non-dimensional time, to let the oscillations vanish.

The LCE estimates are compared in Fig. 2 with the corresponding values obtained using the Floquet theory in[7] for a range of advance ratio $0 \leq \mu \leq 1.5$. The results are in good agreement.

3.2 Helicopter Ground Resonance with Dissimilar Lead-Lag Dampers

Helicopter Ground Resonance is a mechanical instability associated with the in-plane degrees of freedom of the rotor.[8] The combination of the in-plane motion of the blades causes an overall in-plane motion of the rotor center of mass which couples with the dynamics of the airframe and undercarriage system. For this reason, the damping of the in-plane motion of the blades is essential and is usually provided by lead-lag dampers. The problem has been studied using models

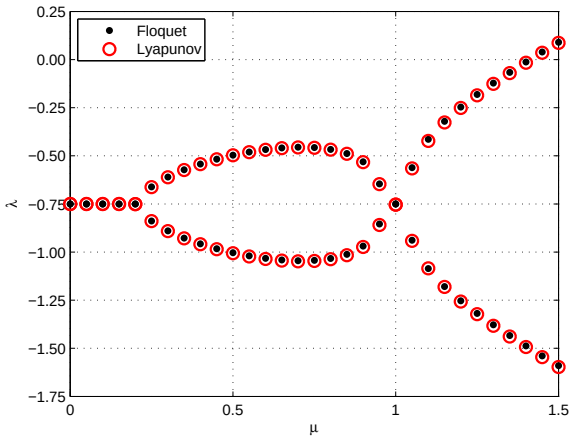

Figure 2: Blade flapping: estimates of LCEs for a range of advance ratio μ.

with various complexity levels. Hammond's model[9] has been extensively used due to its simplicity; as such, it is chosen as the helicopter ground resonance model in this study.

Using multi-blade coordinates, Hammond's model is not periodic for a symmetric rotor (i.e. with identical, equally spaced blades); hence, its stability can be analyzed as a LTI system. Whenever the symmetry of the rotor is broken, time dependence surfaces. A typical case of engineering interest is that of one blade damper inoperative. This is not a normal operating condition; yet, it needs to be analyzed to assess stability, especially for soft in-plane rotors. The equations of motion in the rotating reference frame can be written as

$$\mathbf{M}_r(t)\ddot{\mathbf{q}}_r + \mathbf{C}_r(t)\dot{\mathbf{q}}_r + \mathbf{K}_r(t)\mathbf{q}_r = \mathbf{0} \tag{21}$$

where $\mathbf{q}_r$, $\mathbf{M}_r$, $\mathbf{C}_r$ and $\mathbf{K}_r$ are degrees of freedom vector and mass, damping and stiffness matrices in rotating frame with periodic terms as given in original work.[9] In Hammond's model there are 4 blade lag degrees of freedom (ζ_i, i being blade index) and 2 hub in-plane degrees of freedom, x being longitudinal and y being lateral. Therefore,

$$\mathbf{q}_r = [\zeta_1 \;\; \zeta_2 \;\; \zeta_3 \;\; \zeta_4 \;\; x \;\; y]^T \tag{22}$$

where $\psi_i = \psi + i2\pi/N$ is the azimuth angle of the corresponding blade with blade index i, whereas ψ is the reference azimuth angle. The parameter values are reported in Table 1.

The degree of freedom vector and matrices can be transformed into the non-rotating frame using transformation matrix $\mathbf{T}_1$, its first time derivative $\mathbf{T}_2$ and second time derivative $\mathbf{T}_3$, normalized with the angular speed of the rotor, Ω.[10]

Table 1: Ground resonance: numerical values of Hammond model parameters[9]

Number of blades, N	4
Blade mass moment, S_b	189.1 kg m
Blade mass moment of inertia, J_b	1084.7 kg m^2
Lag hinge offset, e	0.3048 m
Lag spring, k_b	0 N m rad^{-1}
Lag damper, c_b	4067.5 N m s rad^{-1}
Hub mass, m_x, m_y	8026.6 kg, 3283.6 kg
Hub spring, k_x, k_y	1240481.8 N m^{-1}, 1240481.8 N m^{-1}
Hub damper, c_x, c_y	51078.7 N s m^{-1}, 25539.3 N s m^{-1}

$$\mathbf{T}_1 = \begin{bmatrix} 1 & \cos(\psi_1) & \sin(\psi_1) & -1 & 0 & 0 \\ 1 & \cos(\psi_2) & \sin(\psi_2) & 1 & 0 & 0 \\ 1 & \cos(\psi_3) & \sin(\psi_3) & -1 & 0 & 0 \\ 1 & \cos(\psi_4) & \sin(\psi_4) & 1 & 0 & 0 \\ 0 & 0 & 0 & 0 & 1 & 0 \\ 0 & 0 & 0 & 0 & 0 & 1 \end{bmatrix}, \tag{23}$$

$$\mathbf{T}_2 = \frac{\mathrm{d}\mathbf{T}_1}{\mathrm{d}\psi}, \quad \mathbf{T}_3 = \frac{\mathrm{d}\mathbf{T}_2}{\mathrm{d}\psi}.$$

The degrees of freedom vector in non-rotating frame is

$$\mathbf{q}_{nr} = \mathbf{T}_1^{-1}\mathbf{q}_r = [\zeta_0 \;\; \zeta_{1c} \;\; \zeta_{1s} \;\; \zeta_{N/2} \;\; x \;\; y]^T; \tag{24}$$

$\mathbf{q}_{nr}$ includes the collective, ζ_0, cyclic, ζ_{1c} and ζ_{1s}, and reactionless, $\zeta_{N/2}$ blade lead-lag modes, and the two hub displacement modes x and y, as in $\mathbf{q}_r$. It should be noted that, as opposed to the isotropic rotor case in which all dampers are operative, the collective and reactionless modes may also contribute to the dynamics of the rotor when coupled with the hub degrees of freedom so these terms should not be simplified. Then, the equation of motion in the non-rotating frame can be written as

$$\mathbf{M}_{nr}\ddot{\mathbf{q}}_{nr} + \mathbf{C}_{nr}\dot{\mathbf{q}}_{nr} + \mathbf{K}_{nr}\mathbf{q}_{nr} = \mathbf{0} \tag{25}$$

with the corresponding mass $\mathbf{M}_{nr}$, damping $\mathbf{C}_{nr}$ and stiffness $\mathbf{K}_{nr}$ matrices in non-rotating frame which are transformed from the rotating-frame using,

$$\mathbf{M}_{nr} = \mathbf{T}_1^{-1}\mathbf{M}_r\mathbf{T}_1 \tag{26}$$

$$\mathbf{C}_{nr} = \mathbf{T}_1^{-1}(2\Omega\mathbf{M}_r\mathbf{T}_2 + \mathbf{C}_r\mathbf{T}_1) \tag{27}$$

$$\mathbf{K}_{nr} = \mathbf{T}_1^{-1}(\Omega^2\mathbf{M}_r\mathbf{T}_3 + \Omega\mathbf{C}_r\mathbf{T}_2 + \mathbf{K}_r\mathbf{T}_1) \tag{28}$$

In the non-rotating frame, the elements of the matrices do not depend on the azimuth angle, unless the isotropy of the system is spoiled, e.g. by removing or modifying one of the characteristics of the blades such as the lead-lag damper or spring restraint. The estimation of LCEs is illustrated removing the damper from one blade, and by considering the rotor angular speed as the parameter. Since the model has 12 states, only the most critical damping level is shown for clarity. Fig. 3 illustrates the results of the periodic rotor in which one damper is removed. The estimated LCEs match well with the results obtained using the Floquet theory.[7,9] Fig. 4 presents the time evolution of LCE estimates for $\Omega = 400$ rpm: the top plot starts from the time when the system is initially perturbed and the bottom one zooms the behavior for a large enough value of t. The first LCE shows an oscillating behavior and converges to the value given in the plot at the bottom of Fig. 4.

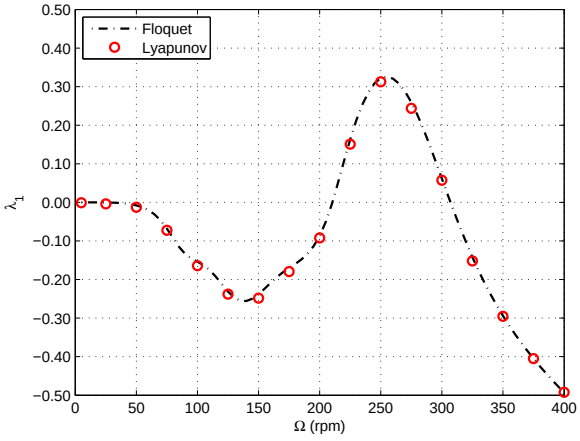

Figure 3: Helicopter ground resonance with one blade damper inoperative: estimate of the largest LCE with a range of rotor angular speed Ω.

3.3 Helicopter Ground Resonance with Non-Linear Lead-Lag Dampers

A distinctive advantage of LCEs is their capability to analyze the stability of non-linear, non-autonomous dynamical systems. Helicopter rotors presents the general characteristics of non-linearity and time dependence.[11] Among non-linear phenomena, limit cycle oscillations (LCO) are defined as isolated closed trajectories of non-linear dynamical systems; when an LCO develops, the system oscillates in a self-sustained man-

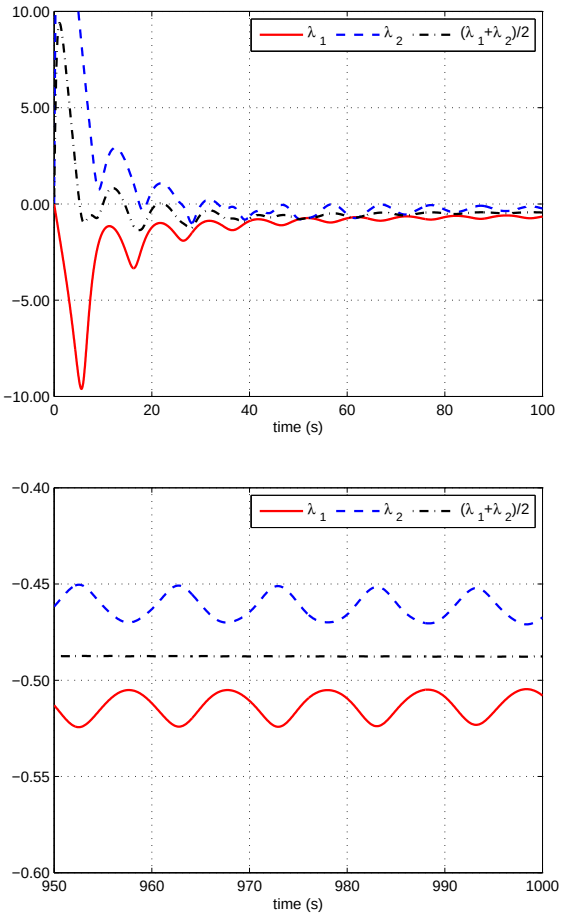

Figure 4: Helicopter ground resonance with one blade damper inoperative: time evolution of estimates of the two largest LCEs ($\Omega = 400$ rpm), time history after start (top) and zoomed view after convergence (bottom).

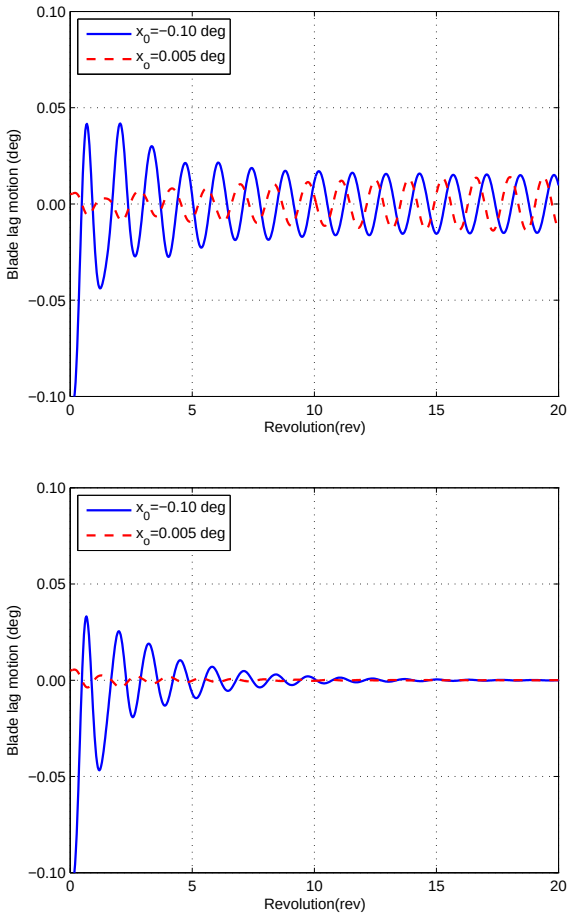

Figure 5: Helicopter ground resonance with nonlinear blade damper: blade lag motion starting from different initial conditions, LCO ($c_L = 0$, top) and exponentially stable ($c_L = c_b$, bottom)

ner without the need of an external input.[12] Clearly, the occurrence of LCOs can effect material life, flight safety and ride comfort of a rotorcraft; their possibility can only be detected if the system is considered non-linear.

For this purpose the same ground resonance model of the previous example is studied with a non-linear lead-lag damper formulation in order to verify the application of the proposed formulation to a non-linear problem. The constitutive law of the non-linear damper model given in Ref.[13] is modified by adding also a linear term to the quadratic term and given as,

$$f_d = \begin{cases} \mathcal{X}\dot{\zeta}|\dot{\zeta}| + c_L\dot{\zeta} & \dot{\zeta} < \dot{\zeta}_L \\ \bar{\mathcal{X}}\dot{\zeta}_L|\dot{\zeta}_L| & \dot{\zeta} \geq \dot{\zeta}_L \end{cases} \tag{29}$$

where $\mathcal{X} = \bar{\mathcal{X}} - c_L/\dot{\zeta}_L$ to ensure that the value of damping at the discontinuity point $\dot{\zeta}_L$ remains the same when the slope c_L is changed. The slope is chosen as the parameter for investigating change of LCE estimates with respect to a parameter, and is expressed as a percentage with respect to the nominal linear damper c_b, having the value given in Table 1. The same parameter values given in Ref.[13] are used for the other parameters and given in Table 2.

In the model of Ref.[13] there is no linear damping, hence the slope c_L is zero. As a result Limit Cycle Oscillations (LCO) are observed. Without the linear term, the model is not realistic, since flow in a hydraulic damper tends to be laminar at small flow rates. Thus, the linear term better describes the physics of the device in the low speed regime. Indeed, this problem has been selected to obtain a LCO in an otherwise reasonably realistic model and to test LCE estimation with a

Table 2: Ground resonance: saturated hydraulic damper parameters.

$\mathcal{X}$	1.2203×10^6	N m s^2 rad^{-2}
$\dot{\zeta}_L$	1.0	deg s^{-1}

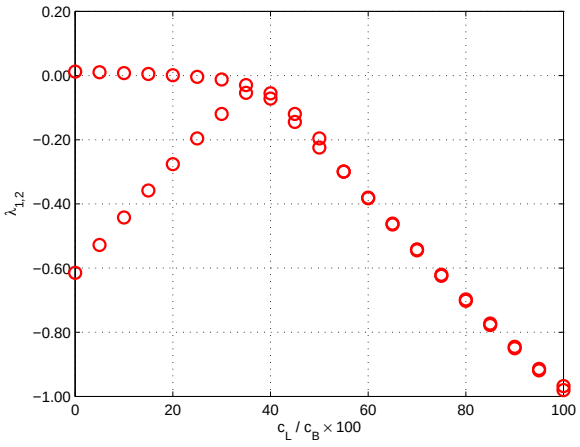

Figure 6: Helicopter ground resonance with nonlinear blade damper: first two LCE estimates for a range of damper slope at zero lag rate c_L.

non-linear problem that may include LCO, exponential stability, and unstable equilibria.

First of all, the blade lag motion (only one of four blades is shown for clarity) is discussed. Fig. 5 shows the blade lag motion for the cases in which the blade experiences LCO ($c_L = 0$, top) and exponential stability ($c_L = c_b$, bottom). In both plots, the simulations start from different initial conditions; one of them has amplitude smaller than that of the expected LCO, whereas the other one is greater, to assess the LCO nature of the attractor by starting from inside and outside the expected periodic orbit. In the plot at the top of Fig. 5, curves with the same amplitude and period are obtained, although a time shift can be observed, thus confirming the limit cycle interpretation of the attractor. It is worth noticing that $\zeta = 0$ is also an equilibrium solution. However, since solutions obtained with initial conditions in the vicinity of $\zeta = 0$ converge to the previously mentioned limit cycle, the solution $\zeta = 0$ is topologically an unstable equilibrium point, a so-called *repellor*. The instability of such solution is confirmed by the present analysis, which estimates a positive LCE. In the plot at the bottom of Fig. 5, the resulting curves converge to $\zeta = 0$, confirming the interpretation of the attractor as a stable point.

If the system has a periodic attractor, a so-called LCO, zero-valued LCE estimates are expected[14] (or very close to zero from a numerical analysis point of view). In order to see this and also further investigate the trends, LCEs are estimated for a range of damper slope at zero lag rate, c_L ($c_L = 0$ was used in Ref.[13]). Results are shown in Fig. 6; as it can be observed, starting from $c_L = 0$ the largest LCE is zero and remains approximately zero until $c_L \approx 0.35 c_b$. Hence, a LCO occurs in this range after the system encounters a perturbation. For larger values of c_L, the two

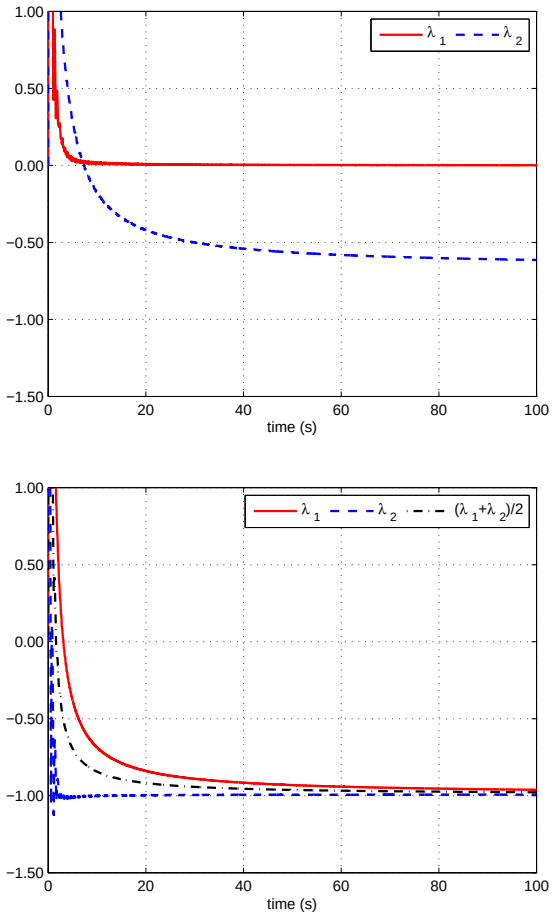

Figure 7: Helicopter ground resonance with nonlinear blade damper: time evolution of LCE estimates, LCO ($c_L = 0$, top) and exponentially stable ($c_L = c_b$, bottom)

largest LCEs (nearly) merge (i.e. they become quite close from a numerical point of view) and the system becomes exponentially stable with all LCEs negative. This is verified by looking at the lag motion of the blade, as given in Fig. 5: in the plot at the top, which corresponds to $c_L = 0$, the blade motion converges to a stable LCO with magnitude 0.015 deg, as reported in Ref.[13] Increasing the zero lag rate slope provides asymptotic stability: for example, when $c_L = c_b$, all LCEs are negative; as shown in the plot at the bottom of Fig. 5, the motion is exponentially stable.

The time evolution of LCE estimates corresponding to the cases of Fig. 5 is shown in Fig. 7. In the case resulting in an LCO, ($c_L = 0$, plots at the top of Fig. 5 and Fig. 7), the first two LCE estimates are distinct. The first LCE, λ_1, quickly converges to zero, corresponding to the stable LCO with magnitude 0.015 deg. Since zero-valued LCE indicates an LCO, the LCE estimates and the time simulations are in agreement. Increasing the slope at zero lag rate provides stability; for a sufficiently large value of c_L, as shown in the plots at

the bottom of Fig. 5 and in Fig. 7, the first two LCE estimates converge to the same value, suggesting that they are coincident, with multiplicity 2, as if they were associated with complex conjugate eigenvalues in a LTI system. This solution is stable, as observed from the time simulations and indicated by the negative largest LCEs.

4. CONCLUSIONS

The estimation of Lyapunov Characteristic Exponents (LCE) to investigate the stability of trajectories of increasingly complex problems is presented and applied to rotorcraft-related problems. The method is illustrated in relation with two periodic and one nonlinear problem related to rotorcraft dynamics. Results are found in good agreement with Floquet theory for LTP problems and verified by time simulation for nonlinear problem.

It is believed that for rotorcraft applications time dependence, often in conjunction with non-strict periodicity and quasi-periodicity, as well as non-linearity cannot be neglected in many applications. Lyapunov Characteristic Exponents provide a quantitative way of measuring stability of trajectories of such systems. LCEs correspond to the real part of eigenvalues for LTI systems, and to Floquet multipliers for LTP systems; hence, they represent a natural generalization of stability indicators that are familiar in current engineering practice, and can proficiently support the analysis of systems with increasing levels of complexity.

References

[1] L. Ya. Adrianova. *Introduction to Linear Systems of Differential Equations*, volume 146 of *Translations of Mathematical Monographs*. American Mathematical Society, Providence, Rhode Island, 1995.

[2] Giancarlo Benettin, Luigi Galgani, Antonio Giorgilli, and Jean-Marie Strelcyn. Lyapunov characteristic exponents for smooth dynamical systems and for Hamiltonian systems; a method for computing all of them. part 1: Theory. *Meccanica*, 15(1):9–20, March 1980. doi:10.1007/BF02128236.

[3] Karlheinz Geist, Ulrich Parlitz, and Werner Lauterborn. Comparison of different methods for computing Lyapunov exponents. *Progress of Theoretical Physics*, 83(5), May 1990. doi:10.1143/PTP.83.875.

[4] Pierangelo Masarati. Estimation of Lyapunov exponents from multibody dynamics in differential-algebraic form. *Proc. IMechE Part K: J. Multi-body Dynamics*, 227(4):23–33, 2012. doi:10.1177/1464419312455754.

[5] C. S. Hsu. On approximating a general linear periodic system. *Journal of Mathematical Analysis and Applications*, 45(1):234–251, 1974.

[6] David A. Peters, Sydnie M. Lieb, and Loren A. Ahaus. Interpretation of Floquet eigenvalues and eigenvectors for periodic systems. *Journal of the American Helicopter Society*, 56(3):1–11, July 2011. doi:10.4050/JAHS.56.032001.

[7] Aykut Tamer and Pierangelo Masarati. Periodic stability and sensitivity analysis of rotating machinery. In *IFToMM ICORD 2014*, Milan, Italy, September 22–25 2014.

[8] Gareth D. Padfield. *Helicopter Flight Dynamics: The Theory and Application of Flying Qualities and Simulation Modelling*. AIAA Education Series, 1996.

[9] C. E. Hammond. An application of Floquet theory to prediction of mechanical instability. *Journal of the American Helicopter Society*, 19(4):14–23, 1974. doi:10.4050/JAHS.19.14.

[10] G. Bir. Multiblade coordinate transformation and its application to wind turbine analysis. In *ASME Wind Energy Symposium*, Reno, Nevada, January 7–10 2008. NREL/CP-500-42553.

[11] Richard L. Bielawa. *Rotary Wing Structural Dynamics and Aeroelasticity*. AIAA, Washington, DC, 2005.

[12] Steven H. Strogatz. *Nonlinear Dynamics and Chaos*. Perseus Books, Reading, Massachusetts, 1994.

[13] Giuseppe Quaranta, Vincenzo Muscarello, and Pierangelo Masarati. Lead-lag damper robustness analysis for helicopter ground resonance. *J. of Guidance, Control, and Dynamics*, 36(4):1150–1161, July 2013. doi:10.2514/1.57188.

[14] L. Dieci, R. D. Russell, and E. S. Van Vleck. On the computation of Lyapunov exponents for continuous dynamical systems. *SIAM Journal on Numerical Analysis*, 34(1):402–423, 1997. doi:10.1137/S0036142993247311.

COPYRIGHT STATEMENT